Bromine and iodine excitation-function measurements with protons and deuterons at 3–17 MeV

H. I. West, Jr., R. M. Nuckolls, B. Hudson, B. Ruiz, R. G. Lanier, and M. G. Mustafa
University of California, Lawrence Livermore National Laboratory, Livermore, California 94551
(Received 10 August 1992)

We report nuclear excitation functions for the reactions ^{79}Br[$(p,n)+(d,2n)$]^{79}Kr, ^{81}Br[$(p,n)+(d,2n)$]^{81}Br, ^{81}Br$(d,p)^{82}$Br, and ^{127}I[$(p,n)+(d,2n)$]^{127}Xe. The measurements were made from reaction threshold to 17 MeV with the Lawrence Livermore National Laboratory's Tandem Van de Graaff accelerator using the stacked-foil method. The ^{79}Br$(d,2n)^{79}$Kr and the ^{81}Br excitation functions are the first reported. The targets consisted of the halides dispersed in the plastic Kapton. The activated targets were assayed using γ counting and mass spectrometry. We found that we had to remeasure the gamma intensities for the ^{79}Kr decay. The excitation functions were modeled using the Hauser-Feshbach statistical-model code STAPRE, using the exciton preequilibrium model. We found a preference for the back-shifted (BS) level density prescription over the use of the Gilbert-Cameron prescription. For BS, the constant K, governing the transition to equilibrium, was taken as 500 to 700 MeV^3. These values gave preequilibrium fractions consistent with those we obtained from ion-recoil range studies of light ion reactions. In general the modeling agreed well with experiment. For the deuteron induced reactions, we had to allow for deuteron breakup using a microscopic breakup fusion approach developed by Udagawa and Tamura. Our analysis of the stripping reaction, ^{81}Br$(d,p)^{82}$Br, by this procedure is especially noteworthy.

PACS number(s): 23.20.Lv, 24.50.+g, 24.60.Dr, 24.60.Gv

I. INTRODUCTION

To meet the programmatic needs of our laboratory, we required accurate measurements of the excitation functions of ^{79}Br[$(p,n)+(d,2n)$]^{79}Kr and ^{127}I[$(p,n)+(d,2n)$]^{127}Xe. Both ^{79}Kr and ^{127}Xe have decay times that lend themselves to the method of measurement in which one irradiates stacks of foils and counts the induced activities off line. Before starting measurements we evaluated the results in the literature [1] using the Hauser Feshbach statistical code STAPRE [2]. In the course of the work, we extended our measurements to ^{81}Br$(p,n)^{81}$Kr, ^{81}Br$(d,2n)^{81}$Kr, and ^{81}Br$(d,p)^{82}$Kr. The decay half-life of ^{81}Kr is 2.1×10^5 yr; thus, we used mass spectrometry to assay the targets for the important krypton reaction products.

For earlier work on ^{79}Br$(p,n)^{79}$Kr, we cite the work of Collé and Kishore [3], Dikšić *et al.* [4], and Sakamoto, Dohniwa, and Okada [5]. The latter two sets of data are the results of high-energy irradiations of a thick array of stacked foils. The results of Weinrich and Kneiper [6] claim general agreement with the rest, but no numbers are given. The results of Collé and Kishore seemed to be the best available. Their results were obtained using thin deposits of KBr on thin aluminum backings to a density of 2–3 mg/cm^2 encapsulated in heat-sealable Mylar. The targets were irradiated using the Brookhaven Van de Graaff accelerator. No prior experimental work was found in the literature for ^{79}Br$(d,2n)^{79}$Kr, ^{81}Br[$(p,n)+(d,2n)$]^{81}Kr, or ^{81}Br$(d,p)^{82}$Br.

For ^{127}I$(p,n)^{127}$Xe, we note the work of Collé and Kishore [3]. In their studies they used targets of KI prepared in the same manner as they used for bromine. In addition, we note the work of Sakamoto, Dohniwa, and Okada [5] and Lagunas-Solar *et al.* [7]. These two sets of measurements were made using thick targets.

For ^{127}I$(d,2n)^{127}$Xe, we cite the work of Balestrini [8]. They used mass spectrometry to assay the targets for ^{127}Xe. Weinreich, Schult, and Stocklin [9] report measurements in general agreement with that of Balestrini.

In the following we first discuss our method of target preparation. We used the stacked-foil method of cross-section measurement. In the interest of accuracy, we limited the number of target foils in an irradiation from 1 to 4. Subsequent runs overlapped in energy. The method of correcting for energy loss in the foils is discussed. Despite what appeared to be excellent work, we found an error in the I_γ's, expressing the intensity of the γ-ray decay, for the ^{79}Kr decays that were used by Collé and Kishore in their work. We corrected this error using results from proportional counters and mass spectrometry. Finally, we did a Hauser-Feshbach statistical-code analysis using the code STAPRE [2]. The interpretation of the data is very much influenced by our earlier work on chromium [10,11] and yttrium [12] in this mass region. The analysis of the data acquired in those works relied heavily upon the advances in nuclear modeling made by Udagawa, Kim, and Tamura [13]. The Q values of the reactions of interest here are listed in Table I.

II. EXPERIMENTAL PROCEDURE AND DATA REDUCTION

Elemental bromine and iodine are difficult to use as accelerator targets. In addition, the reaction products are noble gases that need to be contained or collected for radiation counting. Our previous success in making targets of Eu_2O_3 embedded in the plastic Kapton suggested that

TABLE I. Q values of reactions.

Reactions	Q[a] (MeV)
^{79}Br$(p,n)^{79}$Kr	−2.407
^{79}Br$(d,2n)^{79}$Kr	−4.631
^{81}Br$(p,n)^{81}$Kr	−1.063
^{81}Br$(d,2n)^{81}$Kr	−3.287
^{81}Br$(d,p)^{82}$Br	5.368
^{127}I$(p,n)^{127}$Xe	−1.445
^{127}I$(d,2n)^{127}$Xe	−3.669

[a]Calculated from *Nuclear Wallet Cards* [14].

we choose that approach [15] for halogen targets. We used KBr and KI for the target materials. The selected material was pulverized and mixed with a polymide resin (DuPont RC5057), which when polymerized is the equivalent of Kapton. The mixture was spread out thinly on glass and cured at temperatures up to 260 °C. Targets 25.4 mm in diameter were punched from the sheets produced.

The areal densities of the foils were intercompared by means of fluorescent x-ray spectrometry. Selected foils were chemically assayed to establish the absolute areal densities. The foils were 7–20 mg/cm^2, one-third of which were elemental bromine or iodine.

To ensure noble-gas containment, the target foils were coated with aluminum on both sides to a density of 0.2–0.3 mg/cm^2. (The coating also ensured that those reaction ions that recoiled out the back of the target foils would be contained.) To further ensure there was no gas loss, we found it necessary to keep the beam heat loading in the foil relatively low. To help in this respect, we rastered the beam on the target over an area $\sim$1 cm^2. In general, even though cooling was provided, we found it desirable to keep the heat dissipation less than 0.5 W per target foil. The problem we encountered with overheating was not due to damage to the Kapton foil, but rather separation of the aluminum cladding from the foils; keeping the heat loading low prevented this. To further guard against the possible slow loss of gas during counting, the irradiated targets were encapsulated in thin aluminum containers immediately after irradiation.

The irradiations were carried out using the Lawrence Livermore National Laboratory's (LLNL) Tandem Van de Graaff. The accumulated charge during an irradiation was measured using a digital integrator, Ortec model 439, having an absolute accuracy of ±0.2%.

Gamma counting the target foils was carried out using the automated germanium counters in our laboratory and the results analyzed using the code GAMANAL [16]. The counters are carefully maintained and calibrated. Despite this care, results from different counters could often differ by a percent or so. To minimize this uncertainty, we used the average of results from three counters for each target. We believe the error for a given counter to be less than ±2%, with the average from three counters somewhat less.

TABLE II. ^{127}Xe I_γ's.

γ energy (keV)	Collé and Kishore[a]	Gehrke and Helmer[b]	LLNL
172.1	0.247(10)	0.255(8)	0.2535(80)
202.8	0.681(13)	0.683(4)	0.6830(40)
374.99	0.174(10)	0.172(5)	0.1761(50)

[a]Reference [17].
[b]Reference [18].

A. ^{127}Xe I_γ's

The half-life [8] used for ^{127}Xe was 36.4 d. The I_γ's we used in the data analysis of the iodine data are listed in Table II.

In our case (LLNL), we made relative measurements of the intensities of the indicated γ's and normalized them to the results of Gehrke and Helmer [18] for the most intense γ. Collé and Kishore [17] used gas proportional counting to determine the decay rate of their sources, whereas Gehrke and Helmer used a radiation source calibrated for absolute decay at the National Bureau of Standards. The indicated γ rays were then counted by these workers, respectively, using carefully calibrated germanium γ-ray spectrometers. We have made proportional counter measurements on two of our targets, which, along with our γ counting, seem to confirm the absolute measurements of the earlier workers. We have also made mass-spectrometer measurements (discussed later) in agreement with these earlier workers.

B. ^{79}Kr I_γ's

The half-life used for ^{79}Kr was 35.04 h. We encountered a problem with the I_γ's to be used for the ^{79}Kr decay. We found that the I_γ's determined using internal proportional-counter measurements for absolute decay as given in the literature [17] conflicted with our results using both mass spectrometry and proportional counters for absolute determinations. If we use the results in the literature, in which I_γ for the 261-keV γ is 0.127, we have the first three columns for I_γ in Table III.

Using the I_γ's of the other two γ rays of Collé and Kishore in the decay (397.5 and 606.1 keV) in comparison to the energy dependence determined from corresponding LLNL data normalized to 0.127 (LLNL^c) we obtain $I_\gamma(261)=0.1247$. This assumes that the three I_γ's of Collé and Kishore are independent measurements except for the proportional-counter measurements. The other two LLNL^c values can then be adjusted accordingly. We point out that the relative values from LLNL^c were determined from a large number of counts on several counters. Copper absorbers of areal density 0.475 mg/cm^2 were used, and this along with the geometry used assured that γ-γ and x-γ coincidence summing's were negligible. Also, as mentioned earlier, each target was counted on three counters.

Another approach to determining the I_γ's is to do a detailed balance of the intensities of the transitions in the decay scheme. Since the ^{79}Kr decays to the ground state ($\frac{1}{2}^-$-$\frac{3}{2}^-$) and to the second excited state ($\frac{1}{2}^-$-$\frac{3}{2}^-$) at 261

TABLE III. ^{79}Kr I_γ's.

γ energy (keV)	Collé and Kishore[a]	NDS[b]	LLNL[c]	LLNL[d]	LLNL[e]	LLNL[f]	LLNL[g]
261.3	0.127(4)	0.127	0.127	0.1247	0.1194	0.1186	0.1178(20)
397.5	0.095(3)	0.0933	0.09265				0.0859(17)
606.1	0.081(2)	0.0812	0.07829				0.0726(16)

[a]Reference [17].
[b]Values used by evaluators in *Nuclear Data Sheets* [19].
[c]Our data normalized to 0.127.
[d]Our data normalized to all three γ's of Collé and Kishore using ratio and weights in column 2.
[e]From detailed balance of decay scheme.
[f]From proportional-counter measurements at LLNL.
[g]Average between proportional-counter and mass-spectrometer measurements. We used these I_γ's in subsequent work.

keV are allowed, the respective capture to positron ratios can be calculated to a few percent. There is no decay to the first excited state at 217 keV ($\frac{1}{2}^-$-$\frac{5}{2}^-$). Since the sum of the positron decay to the other two states is readily determined through the detection of the annihilation radiation, we can do a detailed balance of the feeding and decaying of the levels and thereby determine $I_\gamma(261)$. For calculating E_c/β^+, we used Table 5.42 of Wapstra, Nijgh, and Van Lieshout [20], including their method of interpolation. The table is based on the work of Zweifel [21]. We used the decay scheme in Nuclear Data Sheets [19] with γ-intensity values taken from the average of a number of our experimental runs. We obtained $I_\gamma(261)=0.1194(36)$. Possibly, the most uncertain value used in the calculation is E_c/β^+ to the ground state determined from theory. Fortunately, the resultant error in I_γ from this cause is only 60% of the error in E_c/β^+. An earlier evaluation (1966) in Nuclear Data Sheets by Artna [22] gave $I_\gamma(261)=0.114$. We expect that the error of about 4% we assign to our result applies there.

We also made proportional-counter measurements using matched pairs of counters of length L and $L/2$ ($L\approx 40$ cm) [23]. The use of dual counters ensured that accurate end corrections were made. Individual targets were digested by heating to 700 °C for 1 hr in an evacuated vessel. Reactive gases such as H_2, CO_2, N_2, etc., were removed by reactions with hot titanium filaments. The ^{79}Kr was quantitatively transferred to a vessel containing activated charcoal at 77 K. The ^{79}Kr was mixed with a known amount of krypton carrier (measured by weight). The proportional counters were filled with approximately 10 cm^3 STP of the krypton mixture. The pressure of fill was measured with a precision capacitive manometer (MKS-390 HA). Pure methane was then added to a total pressure of 1 atm. The integral discriminator counting thresholds on each counter were set to ~ 50 eV using an ^{55}Fe source and a phase-height analyzer. Sufficient counting data were collected to check the radioactive decay. As a comment, we note that two accelerator runs were made using deuterons of 9.8 and 7.8 MeV producing an appreciable amount of ^{82}Br from the (d,p) reaction. (A negligible amount of ^{82}Br was produced by neutron capture.) ^{82}Br has a half-life of 35.3 h to be compared with that for ^{79}Kr of 35.04 h. We found that if one is overzealous in driving off the ^{79}Kr from the charcoal cold finger that some ^{82}Br will come off (as perhaps HBr) as well thus ruining any attempt to measure ^{79}Kr. From five proportional-counter measurements, along with the respective γ-counter measurements, and using the LLNL[c] I_γ's listed in Table III, we obtained $\sigma_{PC}/\sigma_\gamma=1.070(9)$. This ratio then led to $I_\gamma(261)=0.1186(10)$, in good agreement with the value obtained from the decay scheme detailed balance.

The mass-spectrometry procedures we used are discussed in more detail later. Here we give the results of measurements pertaining to $I_\gamma(261)$ and the calibration used in the assay of targets for ^{81}Kr. After a number of preliminary runs to establish the procedures, four targets were irradiated and counted for ^{79}Kr activity. Two to three days after irradiation, the samples were mass analyzed to determine the number of atoms at end of bombardment. Using $I_\gamma(261)=0.1186$, the results for $\sigma_\gamma/\sigma_{ms}=0.973$. We made similar measurements of iodine targets using the I_γ's of Gehrke and Helmer [18] for ^{127}Xe. Again, after preliminary measurements, we made careful measurements on four targets to obtain $\sigma_\gamma/\sigma_{ms}=0.986$. Gehrke and Helmer consider their I_γ values to be good to 0.5%. That uncertainty along with the uncertainty in γ counting could account for σ_g/σ_m being different from 1.00; also, it may represent a bias in the calibration of the mass spectrometer. Somewhat arbitrarily, we have assumed the latter since doing so results in a reasonable compromise between proportional-counter and mass-spectrometer results. Thus mass-spectrometer data suggest an $I_\gamma(261)=0.1170$. Averaging this value with 0.1186 gives 0.1178. This number is used in the following work. The uncertainty should be less than 2%. The numbers obtained from the decay detail balance were not used in obtaining our value of I_γ, but are consistent with it.

C. Mass spectrometry

The targets that we irradiated and counted for ^{79}Kr and ^{81}Kr activity usually contained enough atoms of ^{81}Kr for mass spectrometry. For targets with $>10^{10}$ atoms, a precision of $\sim 1\%$ was possible. At the 10^9-atom level, the precision of the measurement dropped to $\sim 5\%$.

For the mass spectrometry of krypton, the gas was removed from the target by heating and then received one stage of purification with the same system used for the gas proportional-counter work. Instead of mixing the gas with a large volume of krypton carrier, we used a well-known amount (spike) of almost isotopically pure ^{86}Kr. All of the krypton target gas plus spike was collected on activated charcoal at 77 K. The krypton was released, further purified with hot titanium, and then expanded into the mass-spectrometer volume. The mass-spectrometer entrance valves were closed and the krypton analyzed by standard static noble-gas mass spectrometry. The technique is calibrated by analyzing known quantities of air (1.14 ppm Kr). Air aliquots generally are 0.3 cm^3 STP. The pressure is measured to high accuracy using a capacitive manometer. We believe that the krypton content of the air sample is known to at least 2%. Because we use mono-isotopic spikes of ^{86}Kr and ^{124}Xe, variable additions of air-krypton or air-xenon mixture have no effect on the analysis, unless extremely large amounts of air-krypton or air-xenon mixture are present.

D. ^{82}Br I_γ's

As a result of the deuteron bombardment of bromine, we studied the ^{81}Br$(d,p)^{82}$Br reaction. During irradiation, the foils were surrounded by borated polyethelene; measurements at deuteron energies below 2.0 MeV showed that there was a negligible amount of neutron capture. The half-life used in the analysis was 35.30 h. (This number listed in Lederer *et al.* [24] fits our data much better than the 34.3 h in Nuclear Data Sheets [25]). The γ rays and respective I_γ's used were 554.3 (0.7076), 619.1 (0.4344), and 776.5 (0.8354) keV. These I_γ's were from Nuclear Data Sheets [25]. No effort was expended to check the absolute values of the I_γ's used, but the relative values are consistent to better than 1%.

E. Foil ΔE resolution corrections

Each of our irradiations consisted of one to four target foils interspersed with thin aluminum foils used for energy degraders. Thus it was necessary to calculate accurately the energy loss for the projectiles in each target foil. We have done test experiments from which we find that we can calculate a stack of foils with as much as 3 MeV energy loss (for both protons and deuterons) and keep the error of the loss less than 3%. For most of our measurements, the initial projectile-energy uncertainties were in the 10–50-keV range. However, the accumulated errors in determining the energy in each foil of a stack could vary from 50 to 100 keV. For the lowest-energy points, only one or two foils were used in the stacks and here the reported projectile energies were known to about 20 keV.

Since the energy loss in a target foil could be 1 MeV, especially for deuterons, we had to correct the data for the cross-section variation over the thickness of the foil, in the rising region of the excitation functions. In effect, we must find a function valid at least over the energy range covered by a given foil, which, when integrated over the foil energy loss, gives a number than can be compared to the experimental result. For this deconvolution we use a well-developed procedure [12]. Our fit equations are

$$\ln\sigma(E)=A+B(E-E_T)+C(E-E_T)^2+\cdots$$

and

$$\ln\sigma(E)=A+B\ln(E-E_T)+C\ln^2(E-E_T)+\cdots,$$

in which $\sigma(E)$ is the cross section and E_T the threshold energy. The result of evaluating the equations and the subsequent fit for our ^{127}I$(d,2n)$ data at low energies is shown in Fig. 1.

The energy-resolution correction introduces uncertainties that are difficult to treat without resorting to a formal analysis of the procedure, and this we have not done. The results in Fig. 1 clearly show the correctness of the procedure, and thus the variations from one iteration to the solution to the next, after a sufficient number of iterations, provides an estimate of the error in the fit. Although a fit procedure is used, the corrected data reflect the error in the measurement; that is, the data we report are not smoothed. Implicit in the procedure is the assumption that the true excitation function is smooth, at least when averaged over the region covered by a foil.

Besides the uncertainty in resolution correction, we had several other sources of error. ρ_x, the areal density of the foils, was good to 1–2%. The systematic error in the counter calibration we take to be ±2%. Charge accumulation during irradiation was accurate to ±0.2%. The uncertainties in I_γ's are given in Tables II and III. To these systematic errors the statistical errors were added, all errors added in quadrature.

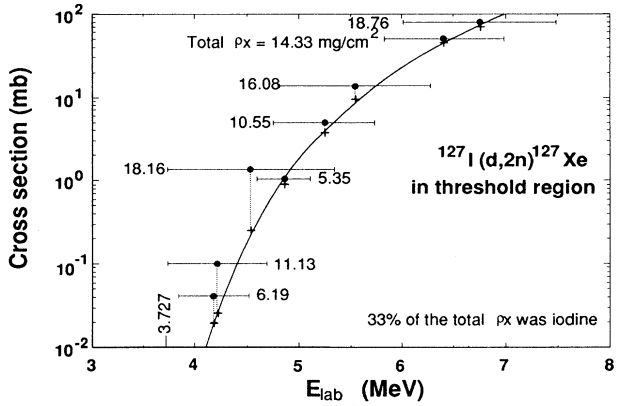

FIG. 1. Energy-resolution corrections to the ^{127}I$(d,2n)^{127}$Xe data in the rising portion of the excitation function. The horizontal bars show the energy range in the respective foils (E_{in} to E_{out}) labeled with the total areal density ρx. The solid circles are plotted at E_{ave}. The pluses are final corrected data obtained by deconvolving the data, as briefly described in the text. The curve is the result of fitting our equation (piecewise continuous) to the corrected data.

TABLE IV. $^{79}Br(p,n)^{79}Kr$ excitation function.

E (MeV)	σ (mb)[a,b]
2.438[c]	0.0
2.48	0.26±0.02
2.80	2.22±0.04
3.17	8.18±0.05
3.47	19.6±0.9
3.94	47.2±1.4
4.53	91.5±2.8
4.88	120.3±3.6
5.55	188.0±5.6
6.29	308.0±9
6.87	360.0±11
6.99	402.0±12
7.05	402.0±12
8.10	520.0±16
8.36	545.0±16
9.06	607.0±18
9.11	628.0±19
9.54	634.0±19
10.06	693.0±21
10.27	670.0±20
10.41	700.0±21
10.98	735.0±22
11.09	704.0±21
11.37	704.0±21
11.74	726.0±22
12.29	684.0±21
12.36	670.0±20
12.96	585.0±18
13.53	502.0±15
14.35	379.0±11
14.66	345.0±10
15.65	238.0± 7
16.87	149.6± 4.5

[a]A 3% systematic error was added in quadrature.
[b]The $\sigma(E)$ was fully corrected for ΔE in the rising portion of the excitation function.
[c]Energy threshold from mass table [14].

III. RESULTS

The results for $^{79}Br(p,n)^{79}Kr$ are give in Table IV and plotted in Fig. 2. In the figure we present our new data along with the results of Collé and Kishore [3], Dikšić *et al.* [4], and Sakamoto, Dohniwa, and Okada [5]. The latter two sets of data are the results of high-energy irradiations of stacked foils. In all cases the data in the literature have been corrected for differences in I_γ. The data of Collé and Kishore were clearly the best currently available in the literature. The agreement between our data and theirs is particularly good except possibly below 5 MeV. The difference there would have to be due to error in energy measurements. The results for $^{81}Br(p,n)^{81}Kr$ are given in Table V and plotted in Fig. 3. No prior data were available. The $^{79}Br(p,n)^{79}Kr$ data are also shown in Fig. 3 for comparison.

We have compared our data with result from the Hauser-Feshbach statistical-model code STAPRE [2]. The

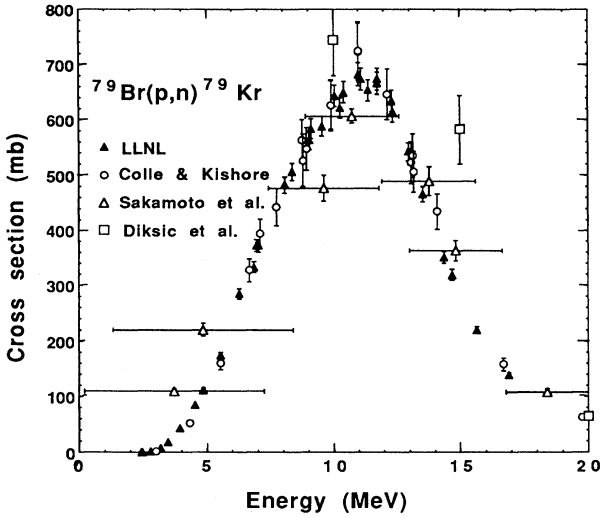

FIG. 2. $^{79}Br(p,n)^{79}Kr$ excitation function. The results of Collé and Kishore [3] agree well with our data. The results of Sakamoto, Dohniwa, and Okada [5] and Dikšić *et al.* [4] from thick stacks of foils are only approximate.

TABLE V. $^{81}Br(p,n)^{81}Kr$ excitation function.

E (MeV)	σ (mb)[a,b]
1.063[c]	0.0
2.23	0.47±0.02
2.80	2.90±0.09
3.17	8.66±0.35
3.94	45.0±1.8
4.53	117.1±4.7
4.88	146.6±5.9
5.55	210.0±8
6.29	359.0±14
6.87	448.0±18
6.99	456.0±18
7.05	429.0±17
8.10	579.0±23
8.36	634.0±25
9.06	660.0±26
9.11	705.0±28
9.54	704.0±28
10.06	724.0±29
10.98	617.0±25
11.09	578.0±23
12.29	434±17
12.36	401.0±16
13.52	278.0±11
14.35	193.3±7.7
15.65	125.4±5.0
16.87	79.7±3.1

[a] $\sigma(E)$ fully corrected for finite ΔE in the rising portion of the excitation function.
[b]A systematic error of 4% was added in quadrature.
[c]Threshold determined from mass table [14].

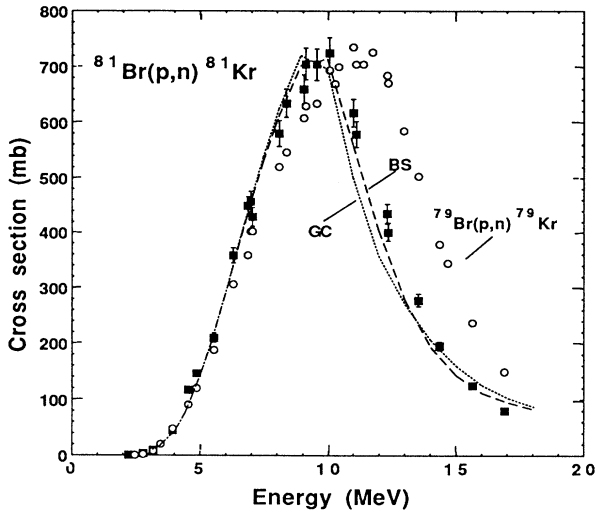

FIG. 3. ^{81}Br$(p,n)^{81}$Kr excitation function plotted along with the ^{79}Br$(p,n)^{79}$Kr excitation function for comparison. STAPRE results are shown for GC, $K=100$, and BS, $K=500$, assuming a 2p-1h initial exciton configuration.

statistical-model code was run with two different level-density prescriptions: that due to Gilbert and Cameron (GC) [26] with parameters from Rose and Cook [27] and a second type, the back-shifted (BS) prescription [28] with the parameters used in the ALICE code [29]. With the BS prescription, we used the level-density parameter $a=A/9$, and pairing shift $\Delta=0$ for an even-even nucleus, $\Delta=-12A^{-1/2}$ for an even-odd nucleus, and $\Delta=-24A^{-1/2}$ for an odd-odd nucleus. We prefer the BS prescription. The STAPRE code allows the use of discrete levels. For the more important branches of the reaction, we have used up to 50 levels taken from Nuclear Data Sheets.

The Hauser-Feshbach analysis treats only the compound part of the reaction. We need to determine the part of the reaction that proceeds through direct interaction (DR) or multistep direct reaction (MSDR) usually called preequilibrium (PE). To estimate these effects, the Livermore version of the STAPRE code uses the exciton model based on the formulas of Williams [30]. The average residual two-body matrix element that appears in the rate expression, determining the transition to equilibrium, is $|M|^2=KA^{-3}E_x^{-1}$. Here A is the atomic number and E_x the excitation energy. To do a calculation, we need the initial particle-hole configuration (here taken as 2p-1h for p,n work), the single-particle level density, $g=(6/\pi^2)a$, and a choice of K. The level-density parameter (a) and the level-pairing shifts (Δ) are taken to be the same as for the Hauser-Feshbach part of the calculation. The parameter K was influenced by our ion-range results [31], following the MSDR and multistep compound (MSC) work of Kalbach [32].

It is worthwhile to point out that the exciton model does not consider angular momentum and parity. It assumes that the preequilibrium cross section is distributed among the levels with different spins and parity in the same proportion as the equilibrium contribution. This limitation may have important consequences for isomer cross sections, but not for the total cross section as presented in this paper. Xiangjun, Gruppelaar, and Akkermans [33] have examined this question in some detail.

In a recent paper [12], we studied the role of DR, considering the one- and two-step processes of Tamura, Udagawa, and Lenske [34] and comparing the results with that from the preequilibrium model. For data from the ^{89}Y$(p,n)^{89}$Zr reaction, a calculation for HF+DR gave good results. With the exciton model, we needed $K=700$ to get equivalent results. Feshbach, Kerman, and Koonin [35] have also provided a MSDR theory. At the one-step level, their result is equivalent to our DR calculation. Kalbach [32] has used the concepts of the MSDR and MSC in the analysis of angular distributions of the reacting particles. She expresses the experimental results in terms of a simple two-parameter equation which nicely fits the data. The term f_{MSD} used there is just the fraction of the total reaction cross section that proceeds through MSD and is equivalent to the preequilibrium fraction (PEF) we normally calculate from STAPRE.

In our recoil-ion range paper [31], we obtained f_{MSD} for a number of reactions. For the purposes here, we use results from ^{89}Y$(p,n)^{89}$Zr and ^{48}Ti$(p,n)^{48}$V. In that paper we made no effort to fit the (p,n) data to derive PEF values, but rather to have $f_{\mathrm{MSD}}=0.0$ at the reaction threshold and approach 1.0 at energies well above the compound peak. Thus, for a fair range at low energies, we let $f_{\mathrm{MSD}}=0.0$, although, in retrospect, the shape of PEF vs. E_{prot} may have been a good compromise. In our judgment a fit of the PEF to our f_{MSD} starting at what would be breakaway from linearity in the range-energy curve extending to 15–18 MeV. We find that the upper range of the bromine data is the most satisfactory in making the comparison. Thus, for the (p,n) data, we use PEF

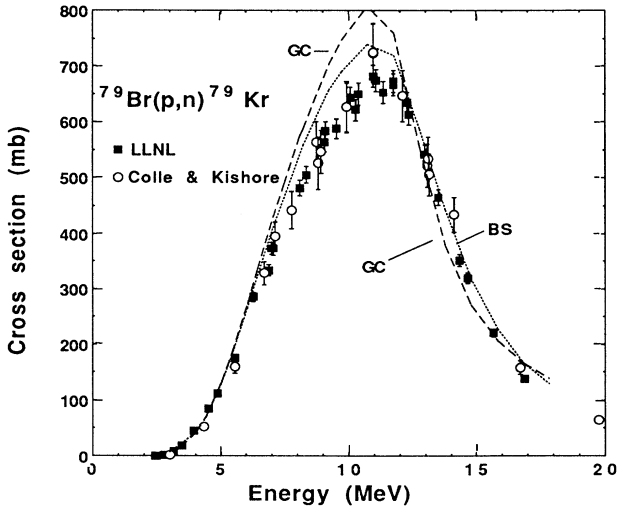

FIG. 4. ^{79}Br$(p,n)^{79}$Kr excitation function, including that of Collé and Kishore [3], compared with STAPRE calculations. We assumed a 2p-1h initial exciton configuration. Calculated results are shown for $K=60$ for GC and $K=500$ for BS.

TABLE VI. $^{79}Br(d,2n)^{79}Kr$ excitation function.

E (MeV)	σ (mb)[a,b]
4.749[c]	0.0
5.04	0.64±0.11
5.09	1.20±0.20
5.19	3.39±0.35
5.50	20.2±0.65
5.51	21.3±0.6
5.93	57.5±1.7
6.05	69.3±2.1
6.23	91.7±2.8
6.53	159.7±4.8
6.85	200.3±6.0
7.32	261.0±8
7.55	317.0±10
7.76	341.0±10
8.67	484.0±15
9.36	576.0±17
9.44	574.0±17
9.77	606.0±18
9.85	627.0±19
10.27	619.0±19
10.87	720.0±22
11.86	722.0±22
12.24	806.0±24
13.20	805.0±24
13.27	805.0±24
13.55	841.0±25
14.46	817.0±25
14.57	883.0±27
15.64	842.0±25
16.75	850.0±26

[a]A systematic error of 3% was added in quadrature.
[b] $\sigma(E)$ is fully corrected for the effects of finite ΔE in the rising portion of the excitation function.
[c]Energy threshold from mass table [14].

TABLE VII. $^{81}Br(d,2n)^{81}Kr$ excitation function.

E (MeV)	σ (mb)[a,b]
3.369[c]	0.0
3.83	0.018±0.009
4.52	14.6±0.9
4.76	32.8±1.5
4.95	42.5±1.7
5.05	60.4±2.4
5.19	79.5±3.2
5.50	124.7±5.0
5.51	127.3±5.1
5.93	191.6±7.7
6.23	247.0±10
6.53	322.0±13
6.85	388.0±16
7.32	444.0±18
7.55	512.0±20
8.67	691.0±28
9.36	745.0±30
9.44	775.0±31
9.85	836.0±33
10.27	841.0±34
10.87	880.0±35
11.86	875.0±35
12.24	950.0±38
13.27	980.0±39
13.55	965.0±39
14.46	911.0±36
14.57	1034.0±41
15.64	895.0±36
16.75	876.0±35

[a] $\sigma(E)$ fully corrected for finite ΔE in the rising portion of the excitation function.
[b]A systematic error of 4% was added in quadrature.
[c]Threshold determined from mass table [14].

$= f_{\mathrm{MSD}} = 0.25$ at about 18 MeV. We find that $K = 500-700$ fits our data well. We also find, as shown later, that this procedure works well for the $(d,2n)$ data, but there the analysis is more complex and we need a different value for f_{MSD}. We have also used the GC prescription, requiring the same final results for the PEF in relation to f_{MSD}. There the value of K varied from 60 to 150, reflecting the difference in the a values in the STAPRE code for the two options. Here the default value is 141. We again emphasize that K is used strictly to set the PEF, in principle, an observable.

The optical potentials we used in the calculations are from Perey and Perey [36] for protons, Moldauer [37] ($E_n < 1$ MeV) and Rapaport [38] ($E_n > 1$ MeV) for neutrons, Daehnick, Childs, and Vrcelj [39] for deuterons, and McFadden and Satchler [40] for alpha particles. These potentials work well in our experience. The $Br(p,n)$ results are shown in Figs. 3 and 4. The parameters used in the fits are given in the captions. In each case we were able to get the best fit to the data using the BS level-density prescription.

The $(d,2n)$ results for ^{79}Br and ^{81}Br are given in Tables VI and VII with plots in Figs. 5 and 6. In Table VIII we give the results of the $^{81}Br(d,p)^{82}Br$ reaction along with a plot in Fig. 7. No prior data were available for these reactions. In general, we find that the calculated excitation functions for $(d,2n)$ reactions are 20–30% larger than the measured values, even though we were careful to use an optical potential appropriate for deuterons. The reason, of course, is the loss of reaction due to an appreciable probability for breakup of the deuteron in the entrance channel. This effect shows up immediately in the value of f_{MSD} we measured in our recoil-ion paper [31]. Typically, we need PEF = 0.4–0.5 at 18 MeV. One approach to treat the breakup problem, due to Udagawa, Kim, and Tamura [13], is somewhat phenomenological and is called the direct-reaction approach to fusion (DRAF). Here we consider the imaginary part of the interaction potential W as the sum of two parts W_F and W_D, where W_F is the fusion potential and W_D is the contribution from direct reaction (DR), break up (BU) of the deuteron, and breakup fusion (BUF). Clearly, W_F and W_D respond to different spin distributions and must be treated separately. We have the following picture:

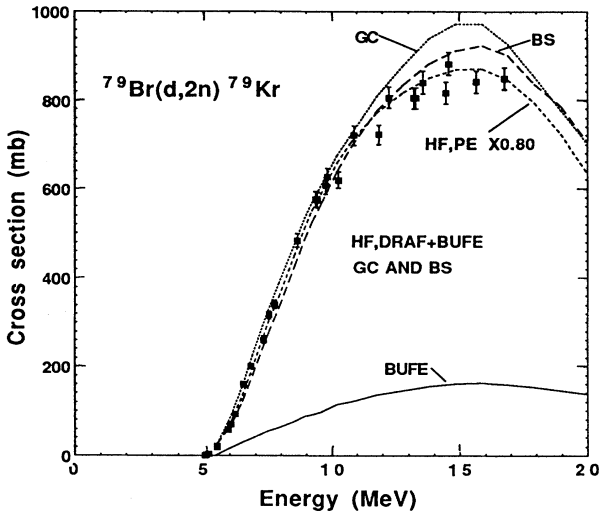

FIG. 5. ^{79}Br$(d,2n)^{79}$Kr excitation function. In the STAPRE modeling, we used a 2p-0h initial exciton configuration, $K=100$ for GC and $K=500$ for BS. The best fit to the data was obtained by using a 20-fm cutoff (equivalent to using the full optical potential) in the calculation and reducing the result by 20%. The other two curves are the result of a microscopic breakup fusion calculation $\sigma_{\rm Th}=\sigma_{\rm HF}^{\rm DRAF}+\sigma_{\rm BUFE}$, using $R_C=8.5$ fm. PEF(18)$_{\rm HF}=0.43$.

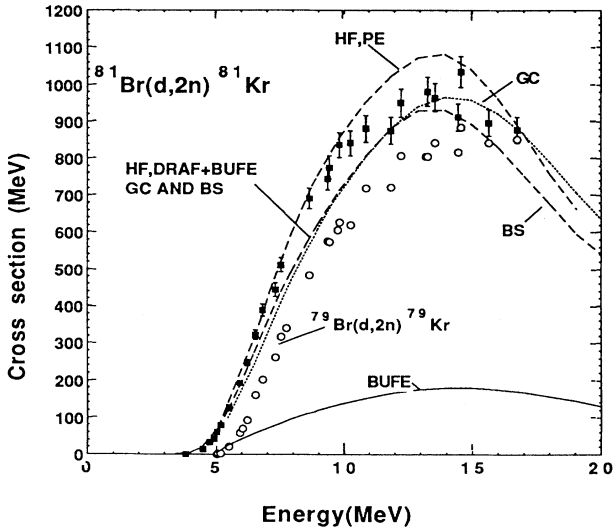

FIG. 6. ^{81}Br$(d,2n)^{81}$Kr excitation function. ^{79}Br$(d,2n)^{79}$Kr results are shown for comparison. STAPRE was run using a 2p-0h initial exciton configuration with $K=100$ for GC and $K=500$ for BS. The upper curve is the result of using a 20-fm cutoff; however, the results were not reduced as in Fig. 5. The other two calculated curves are the results of a microscopic breakup fusion calculation, $\sigma_{\rm HF}^{\rm DRAF}+\sigma_{\rm BUFE}$, with $R_C=8.57$ fm, $K=100$ for GC, and $K=500$ for BS. The results are changed only slightly using $K=125$ for GC and $K=600$ for BS. PEF(18)$_{\rm HF}=0.52$.

TABLE VIII. ^{81}Br$(d,p)^{82}$Kr excitation function.

E (MeV)	σ (mb)[a]
3.83	28.1±0.9
4.20	48.4±1.5
4.52	71.6±2.1
4.76	90.5±2.7
4.95	102.6±3.1
5.06	110.8±3.3
5.19	124.2±3.7
5.50	151.9±4.6
5.51	155.5±4.7
5.93	181.1±5.4
6.05	191.8±5.8
6.23	197.6±5.9
6.52	221.0±7
6.85	236.0±7
7.32	240.0±7
7.55	238.0±7
7.76	239.0±7
8.43	233.0±7
8.67	241.0±7
9.44	224.0±7
9.77	219.0±7
9.85	230.0±7
10.27	204.0±6
10.48	209.0±6
11.86	186.5±5.6
13.20	166.5±5.6
13.37	164.8±5.0
14.46	145.0±4.4
14.57	147.0±4.0
15.64	132.1±4.0
16.75	121.0±3.6

[a]A 3% systematic error was added in quadrature.

$$W_F=\begin{cases} W & \text{for } r<R_C\ , \\ 0 & \text{for } r>R_C\ , \end{cases}$$

$$W_D=W-W_F\ .$$

The cutoff R_C is somewhat larger than the nuclear radius and is a function of the optical potential. It is determined by equating σ_{W_D} to the sum of $\sigma_{\rm BU}+\sigma_{\rm BUF}$. In the DRAF method, the transmission functions T_l are cut off at R_C and the calculation proceeds as a modified Hauser-Feshbach (HF) calculation using the STAPRE code. We also allow for PE emission in the code via the exciton model. Calculations with R_C result in cross sections that underestimate experiment.

To complete the calculation, we need to include the contribution from σ_{W_D} to the reaction channel. This is done from a microscopic calculation $\sigma_{\rm BUF}$, followed by evaporation. We refer to this as $\sigma_{\rm BUFE}$ [41–44]. For the final result, we obtain

$$\sigma_{\rm Th}=\sigma_{\rm HF}^{\rm DRAF}+\sigma_{\rm BUFE}\ .$$

We have had prior experience in using this approach. We studied the ^{52}Cr$(d,2n)^{52}$Mn^{g,m} reactions [10,11].

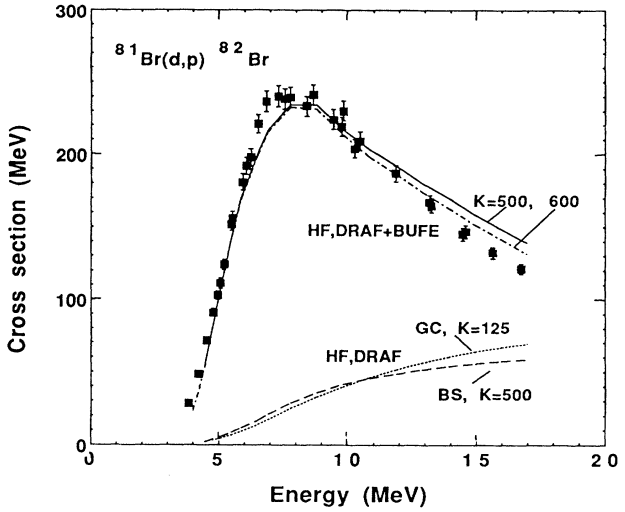

FIG. 7. ^{81}Br$(d,p)^{82}$Br excitation function. The calculation consisted of $\sigma_{\rm HF}^{\rm DRAF}+\sigma_{\rm BUFE}$ and was carried out exactly as was done for the $(d,2n)$ data. For $\sigma_{\rm HF}^{\rm DRAF}$, $R_C=8.57$ fm, and we used 2p-0h. Results for $K=125$ for GC and $K=500$ for BS are shown in the bottom curves. The upper curves include the microscopic part of the calculation. There we used $K=500$ and 600.

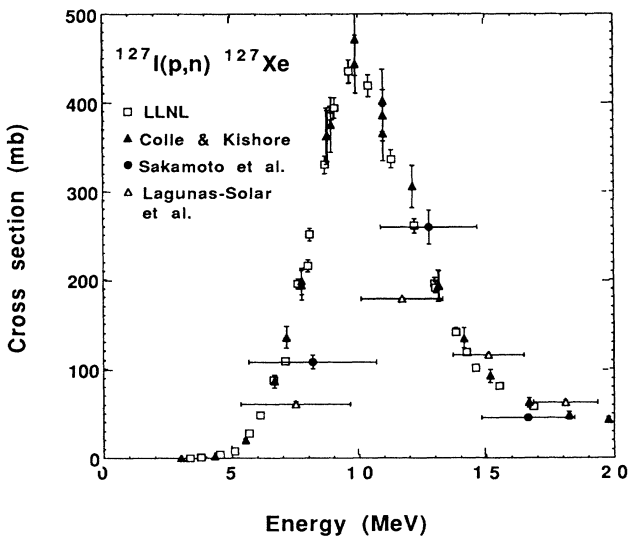

FIG. 8. ^{127}I$(p,n)^{127}$Xe excitation function. The results are compared with earlier measurements of Collé and Kishore [3], Sakamoto, Dohniwa, and Okada [5], and Lagunas-Solar *et al.* [7]. Our data are in good agreement with the Collé-Kishore data.

There the theory was needed to understand experimental values of σ_m/σ_g. We have also studied ^{93}Nb(d,p) angular distributions [45] with good success.

The value of $f_{\rm MSD}$ we obtained from our ion-range analysis is the result of all effects leading to direct reaction and in this case applies to $\sigma_{\rm Th}$. The HF calculation then provides a PEF that needs some correction for comparison to $f_{\rm MSD}$. At 18 MeV the PEF we can expect for the microscopic cross section should be close to 1.0. Thus, considering the values of $\sigma_{\rm BUFE}$, we obtained in our $(d,2n)$ analysis, the HF-PEF will be lower than $f_{\rm MSD}$ by 10–20 %.

A second approach to treating the deuteron breakup problem is that of Baur *et al.* [46]. This model proceeds through a microscopic point of view. In contrast, the University of Texas model of Udagawa and Tamura, as used in our paper, proceeds from a phenomenological approach and is a convenient way of including the optical model in the calculation for the breakup rather than relying on the full microscopic calculation. We have had good success with this approach. The University of Texas group has examined the approach of Bauer *et al.* The differences between the two methods are discussed in [45] and references therein.

A comparison of our modeling calculations with experiment for ^{79}Br$(d,2n)^{79}$Kr and ^{81}Br$(d,2n)^{79}$Kr are given in Figs. 5 and 6. The comparison for the ^{79}Br$(d,2n)^{79}$Kr data is fairly good. The ^{81}Br$(d,2n)^{81}$Kr modeling results are not as successful, but, rather show a significant difference between calculation and experiment in the rising portion of the excitation function. The calculations are sensitive to the optical potential in this region. The modeling results of the ^{81}Br$(d,p)^{82}$Kr data as shown in

TABLE IX. ^{127}I$(p,n)^{127}$Xe excitation function.

E (MeV)	σ (mb)[a,b]
1.456[c]	0.0
3.35	0.126±0.006
3.80	0.482±0.018
4.53	3.43±0.11
5.11	7.90±0.26
5.70	28.4±0.9
6.12	48.6±1.5
6.67	87.4±2.6
7.12	108.4±3.3
7.63	195.4±5.9
8.02	216.0±7
8.10	251.0±8
8.68	330.0±10
8.90	384.0±12
9.09	394.0±12
9.65	435.0±13
10.41	419.0±13
11.30	337.0±10
12.19	261.0± 8
12.98	196.0± 5.9
13.02	191.1± 6.0
13.82	141.1± 4.3
14.25	118.3± 3.6
14.59	101.5± 3.1
15.53	81.0± 2.4
16.84	57.9± 1.8

[a]A systematic error of 3% was added in quadrature to the other errors.

[b]The results $\sigma(E)$ were fully corrected for effects due to finite values of ΔE.

[c]Threshold from mass table [14].

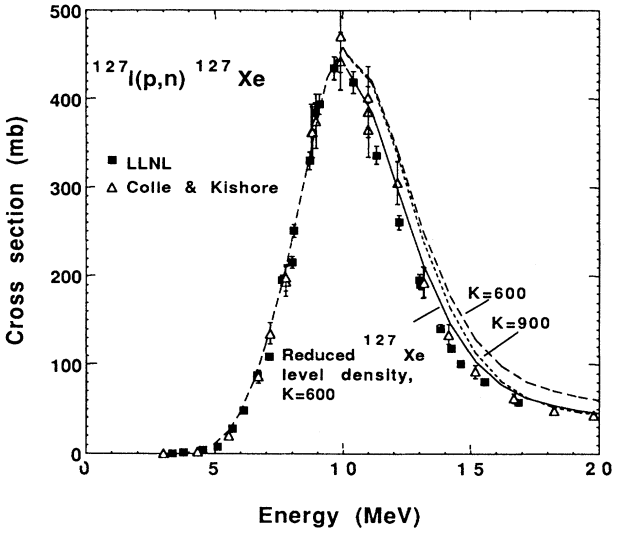

FIG. 9. $^{127}I(p,n)^{127}Xe$ excitation function. We used a 2p-1h initial exciton configuration. The upper curve is from STAPRE using $K=600$. This value of K would appear to be a good choice for a global value. We have PEF(18)=0.21. We get a somewhat better fit for $K=900$ with PEF=0.14. Varying the other parameters one usually varies did not help. The best results were obtained by lowering the level density for ^{127}Xe by 10%; PEF(18)=0.14.

Fig. 7 are very good. We consider this result to be an outstanding success of the procedure. Here we note that the Hauser-Feshbach part of the calculation is small compared to the total. Of course, this result emphasizes the role of stripping in the reaction. It is also significant that the value of K used in PE model is completely consistent with those values used for $(d,2n)$ and, for that matter, for the (p,n) reactions as well.

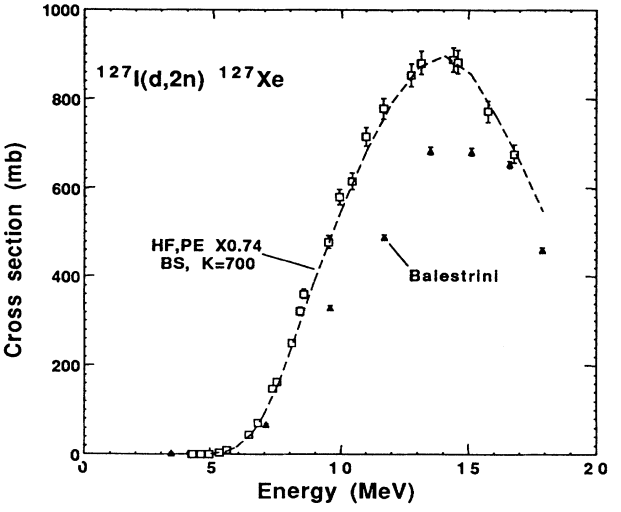

FIG. 10. $^{127}I(d,2n)^{127}Xe$ excitation function compared with results of Balestrini [8]. The theoretical curve is from STAPRE calculations ×0.74. The factor of 0.74 allows for deuteron breakup. The procedure provides a quick estimate of the $(d,2n)$ excitation function.

The results for $^{127}I(p,n)^{127}Xe$ are give in Fig. 8 and Table IX. We present our new data, the experimental results of Collé and Kishore [3]. Sakamoto, Dohniwa, and Okada [5], and Lagunas-Solar *et al.* [7]. For the (p,n) results, we find that our measurements are in good agreement with the results of Collé and Kishore, usually within experimental error.

Figure 9 shows the results of a STAPRE calculation for the $^{127}I(p,n)^{127}Xe$ data using the BS prescription. We consider $K=600$ a global value. Varying all other parameters that one usually changes would not bring the high-energy results into line. We tried $K=900$, but as seen in Fig. 9, the results are not good. However reducing the level density for ^{127}Xe by a nominal 10% greatly improves the fit. However, PE(18 MeV), which equals 0.21 for the more global run, then dropped to 0.14. Possibly at higher A, the PEF should be reduced, suggesting that the A^{-3} dependence of $|M|^2$ needs modifying.

Figure 10 and Table X show the $^{127}I(d,2n)^{127}Xe$ results. We note in the figure that the experimental results of Balestrini [8] are considerably lower than our results. However, for other than the point at low energy, these results scale up to our results by using a factor of about 1.5. Interestingly, the assays of the foils irradiated in their experiment were carried out using mass spectrometry rath-

TABLE X. $^{127}I(d,2n)^{127}Xe$ excitation function.

E (MeV)	σ (mb)[a,b]
3.727[c]	0.0
4.19	0.020±0.002
4.21	0.026±0.004
4.54	0.256±0.057
4.86	0.92±0.03
5.24	3.82±0.15
5.54	9.67±0.31
6.40	44.5±1.4
6.75	71.5±2.2
7.33	147.8±4.5
7.53	163.0±4.9
8.10	250.0±8
8.39	322.0±10
8.56	361.0±11
9.51	479.0±14
9.94	581.0±18
10.43	616.0±19
10.98	715.0±22
11.67	779.0±23
12.73	853.0±26
13.13	882.0±27
14.38	889.0±27
14.55	883.0±27
15.73	772.0±23
16.79	677.0±20

[a]A 3% systematic was added in quadrature.
[b]The results $\sigma(E)$ were fully corrected for effects due to finite values of ΔE.
[c]Threshold calculated from mass table [14].

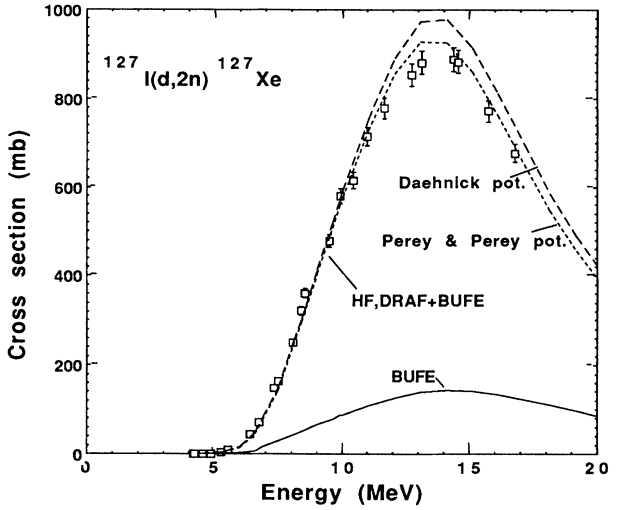

FIG. 11. ^{127}I$(d,2n)^{127}$Xe excitation function including detailed modeling. Results are shown for the optical potential of Daehnick, Childs, and Vrcelj [39] and Perey and Perey [36]. For the first case, $R_C=9.96$ fm, and for the second case, $R_C=9.37$ fm, which are used in establishing the T_l's for STAPRE. We used the BS prescription with $K=600$. PEF(18)$_{HF}=0.35$.

er than the usual γ counting. However, Balestrini used air xenon as a spike and could not determine the extent or effects of air contamination. Our work used separated isotopes of krypton and xenon so that the noble-gas contributions to the air could not affect the results. No other experimental data were available.

For the $(d,2n)$ data of Fig. 10, we also show the result of a STAPRE calculation which has been multiplied by 0.74 to allow for breakup of the deuteron. In applying the breakup fusion calculation to ^{127}I$(d,2n)^{127}$Xe, the calculation did not go as smoothly as for the lighter masses we studied. R_C is deduced from the microscopic calculation and normally varies very little as a function of E_x. For the concept of a two-component cross section to be most effective, R_C should vary little with excitation energy. In this case the variation was more than usual. For the calculation we show the results of using two potentials, Daehnick, Childs, and Vrcelj [39] and Perey and Perey [36]. The results are shown in Fig. 11. Despite our misgivings, the overall results are good.

IV. CONCLUSIONS

We have measured the (p,n) and $(d,2n)$ nuclear excitation functions for targets of ^{79,81}Br and ^{127}I and have compared them with results in the literature. In addition, we measured the stripping reaction ^{81}Br$(d,p)^{82}$Br. The measurements of ^{79}Br$(d,2n)^{79}$Kr and those of ^{81}Br cross sections are the first reported. We obtained a good fit to the (p,n) data using a Hauser-Feshbach analysis (including exciton preequilibrium) using global parameters. For the back-shifted level-density prescription, we used $K=500-700$ MeV^3. The values of K we used gave PEF's consistent with results we obtained from our recoil-ion-range studies.

For the $(d,2n)$ and (d,p) data, we needed to include the effects of deuteron breakup to model the data. For $(d,2n)$ data we can make allowances for deuteron breakup simply by scaling the HF-PE calculations by 0.7–0.8. However, for the (d,p) reaction, the breakup effects dominate the statistical part so that detailed calculations of the breakup effect are required. Of course, the $(d,2n)$ data yield quite nicely to such an analysis. For the ^{127}I$(d,2n)^{127}$Xe results, however, we found that the R_C returned from the microscopic breakup calculation varied with deuteron energy more than normal. This indicates that more study of such calculations is needed before they can be applied universally.

ACKNOWLEDGMENTS

We thank the Van de Graaff crew at LLNL for their help during irradiations. Ruth Anderson was of considerable help during γ-ray counting with the Nuclear Chemistry germanium γ-ray spectrometers. We thank Plastics Shop and Materials Fabrication Division for their help in making the targets. Finally, we thank T. Udagawa and T. Tamura for the use of some of their codes and their interest and cooperation in helping us to learn and to use the DRAF and BUFE procedures. This work was performed under the auspices of the U.S. Department of Energy at the Lawrence Livermore National Laboratory under Contract No. W-7405-ENG-48.

[1] R. G. Lanier, M. G. Mustafa, and H. I. West, Jr., Lawrence Livermore National Laboratory Report No. UCID-21659, 1989.
[2] M. Uhl and B. Strohmaier, Institute fur Radiumforschung und Kernphysik, Vienna, Report No. IRK76/01 (LLNL version updated 1981).
[3] R. Collé and R. Kishore, Phys. Rev. C **9**, 2166 (1974).
[4] M. Dikšić, J.-L. Galinier, H. Marshall, and L. Yaffe, Phys. Rev. C **19**, 1753 (1979).
[5] K. Sakamoto, M. Dohniwa, and K. Okada, Int. J. Appl. Radiat. Isot. **36**, 481 (1985).
[6] R. Weinreich and J. Knieper, Int. J. Appl. Radiat. Isot. **34**, 1335 (1983).
[7] M. C. Lagunas-Solar, O. F. Carvacho, L. J. Harris, and C. A. Mathis, Int. J. Appl. Radiat. Isot. **37**, 835 (1986).
[8] S. J. Balestrini, Phys. Rev. **95**, 1502 (1954).
[9] R. Weinreich, O. Schult, and G. Stocklin, Int. J. Appl. Radiat. Isot. **25**, 535 (1974).
[10] H. I. West, Jr., R. G. Lanier, and M. G. Mustafa, Phys. Rev. C **35**, 2067 (1987).
[11] M. G. Mustafa, T. Tamura, and T. Udagawa, Phys. Rev. C **35**, 2077 (1987).
[12] M. G. Mustafa, H. I. West, Jr., H. O. O'Brien, R. G. Lanier, M. Benhamou, and T. Tamura, Phys. Rev. C **38**, 1624 (1988).
[13] T. Udagawa, B. T. Kim, and T. Tamura, Phys. Rev. C **32**,

123 (1985).
[14] J. K. Tuli, *Nuclear Wallet Cards* (National Nuclear Data Center, Brookhaven National Laboratory, Upton, New York, 1990).
[15] H. I. West, Jr., R. G. Lanier, M. G. Mustafa, R. M. Nuckolls, J. Frehaut, A. Adam, and C. A. Philis, Lawrence Livermore National Laboratory, Livermore, CA, Report No. UCAR 10062-89, 1989, p. 58.
[16] R. Gunnink and J. B. Niday, Lawrence Livermore Laboratory Report No. UCRL 51061, 1972.
[17] R. Collé and R. Kishore, Phys. Rev. C **9**, 981 (1974).
[18] R. J. Gehrke and R. G. Helmer, Int. J. Appl. Radiat. Isot. **28**, 744 (1977).
[19] B. Singh and D. A. Viggars, Nucl. Data Sheets **37**, 461 (1982).
[20] A. H. Wapstra, G. J. Nijgh, and R. Van Lieshout, *Nuclear Spectroscopy Tables* (North-Holland, Amsterdam, 1959), p. 64.
[21] P. F. Zweifel, Phys. Rev. **107**, 329 (1957).
[22] A. Artna, Nucl. Data Sheets **B1-4**, 51 (1966).
[23] N. A. Bonner and R. C. Finkel, Lawrence Livermore National Laboratory Report No. UCID 21538, 1988.
[24] C. M. Lederer, V. S. Shirley, E. Browne, J. N. Dairiki, R. E. Doebler, A. A. Shihab-Elden, L. J. Jardine, J. K. Tuli, and A. B. Buyrn, *Table of Isotopes,* 7th ed. (Wiley, New York, 1978).
[25] H.-W. Muller, Nucl. Data Sheets **50-1**, 29 (1987).
[26] A. Gilbert and A. G. W. Cameron, Can. J. Phys. **43**, 1446 (1965).
[27] E. K. Rose and R. L. Cook, Australian Atomic Energy Commission Report No. AAEC/E419, 1977 (unpublished).
[28] W. Dilg, W. Schantil, H. Vonach, and M. Uhl, Nucl. Phys. **A217**, 269 (1973).
[29] M. Blann and H. K. Vonach, Phys. Rev. C **28**, 1475 (1983).
[30] F. C. Williams, Jr., Phys. Lett. **31B**, 184 (1970); Nucl. Phys. **A166**, 231 (1971).
[31] H. I. West, Jr., M. G. Mustafa, R. G. Lanier, and H. O'Brien, Phys. Rev. C **43**, 1352 (1991).
[32] C. Kalbach, Phys. Rev. C **37**, 2350 (1988).
[33] Shi Xiangjun, H. Gruppelaar, and J. M. Akkermans, Nucl. Phys. **A466**, 333 (1987).
[34] T. Tamura, T. Udagawa, and H. Lenske, Phys. Rev. C **26**, 379 (1982).
[35] H. Feshbach, A. Kerman, and S. Koonin, Ann. Phys. (N.Y.) **125**, 429 (1980).
[36] C. M. Perey and F. G. Perey, At. Data Nucl. Data Tables **17**, 6 (1976). For protons, the second potential on p. 6 was used.
[37] P. A. Moldauer, Nucl. Phys. **47**, 65 (1963).
[38] J. Rapaport, Phys. Rep. **87**, 25 (1982).
[39] W. W. Daehnick, J. D. Childs, and Z. Vrcelj, Phys. Rev. C **21**, 2253 (1980).
[40] L. McFadden and G. R. Satchler, Nucl. Phys. **84**, 117 (1966).
[41] T. Udagawa and T. Tamura, Phys. Rev. C **33**, 494 (1986).
[42] T. Udagawa, X.-H. Li, and T. Tamura, Phys. Rev. C **37**, 429 (1988).
[43] R. C. Mastroleo, T. Udagawa, and T. Tamura, J. Phys. C **15**, 473 (1989).
[44] T. Udagawa, Y. J. Lee, and T. Tamura, Phys. Rev. C **39**, 47 (1989).
[45] R. C. Mastroleo, T. Udagawa, and M. G. Mustafa, Phys. Rev. C **42**, 683 (1990).
[46] G. Baur, F. Rösel, D. Trautmann, and R. Shyam, Phys. Rep. **111**, 333 (1984).